Optimal Precoding Based Spectrum Compression for Faster-Than-Nyquist Signaling

Wen Shan, Liu Guanghui, Chen Qiang, Qu Huiyang and Wang Yanyan

May 30, 2018

Optimal Precoding Based Spectrum Compression for Faster-Than-Nyquist Signaling

Shan Wen, Guanghui Liu, Qiang Chen, Huiyang Qu, Yanyan Wang
University of Electronic Science and Technology of China, Chengdu 611731, P.R. China
Email: guanghuiliu@uestc.edu.cn, {shanwen, qiangchen, hyqu, yywang}@std.uestc.edu.cn

***Abstract*—Faster-than-Nyquist (FTN) signaling is capable of improving the spectral efficiency by offering a higher information rate, while preserving the signaling bandwidth. In this paper, preceding the FTN modulation, a precoding based data spreading is utilized to introduce an artificial interference, which in the frequency domain shapes the signal spectrum and compresses the transmission bandwidth. In this scheme, the spectral efficiency is improved in both time and frequency domains. Further, we optimize the precoder by maximizing the ultimate system capacity and by maximizing the minimum Euclidean distance between the modulated symbols. The spectrum mask limitations are also considered for an imposed constraint on the optimization. Simulation results demonstrate that the 16-ary quadrature amplitude modulation (16-QAM) signaling can achieve the same spectral efficiency as the 64, 256-QAM Nyquist signaling, while the signal-to-noise ratio gains are about 2.5 dB and 5 dB, respectively. Furthermore, the proposed scheme outperforms the existing FTN system in terms of energy performance, noise immunity and boosts the achievable capacity limit of the system subject to the mask.**

***Index Terms*—Faster-than-Nyquist(FTN), partial response signaling (PRS), shaping pulse design, capacity analysis, spectrum mask.**

I. INTRODUCTION

FTN signaling, known as a typical non-orthogonal transmission scheme, can enhance the throughput of the communication link without increasing bandwidth or extra energy consumption [1], [2]. Currently, the efficient modulation scheme has been applied to many communication systems, such as long-haul optical links and satellite broadcasting systems [3]. Also, it is considered as a candidate waveform technology of the fifth generation wireless systems [4].

In 1975, the FTN was proposed by Mazo in [5], of which the symbol duration can be compressed to 80% of that in the Nyquist case without decreasing the *minimum Euclidean distance* between signals, when employing the sinc pulse to transfer binary symbols. Since the asymptotic performance of optimum detection is determined by the minimum distance [2], 25% (i.e., $1/0.8 - 1$) more symbols are transmitted in a given time-window, without deterioration of the bit-error rate (BER) performance. Accordingly, 0.8 is specified as the Mazo limit for the sinc-pulse shaping. In [6], the limits for the family of root raised cosine (RRC) pulses with excess bandwidth β were evaluated. Additionally, according to [7], the higher capacity relative to the Nyquist signaling can be interpreted as utilizing the excess bandwidth of non-sinc pulses. In practice, we can increase the signaling rate by exploiting two approaches: reducing the symbol duration in the time domain and compressing the spectral occupation in the frequency domain [2].

In the FTN system, the Nyquist criterion does not hold any more, then the inter-symbol interference (ISI) is inevitable. A more sophisticated and complex sequence detection algorithm needs to be designed at the receiver end to combat with ISI. In [8], a low-complexity turbo equalization scheme based on the improved M-BCJR algorithms was developed to retrieve the transmitted symbols from the ISI-spoiled observation. Note that the FTN-introduced ISI is basically determined by the shaping pulse, thus a linear pre-equalization scheme [9] at the transmitter was studied for easing the decoding burden at the receiver. By contrast, the precoder in [10] was derived for decreasing the minimum distance reduction, or equivalently improving the BER, at the expense of extra complexity. To summarize, the existing precoders are applied to trade-off between performance and complexity.

Since the FTN signaling with independent and identically distributed (i.i.d.) inputs cannot change the power spectral density (PSD) distribution [7], the spectral efficiency is improved only through packing the data pulses closer in the time domain. In the light of the traditional partial response signaling (PRS) [11], the precoder in this paper, is subtly designed to reduce the bandwidth occupancy for achieving higher bandwidth efficiency, which is different from the precoding schemes in [9], [10]. In the proposed FTN system, the approach improving the spectral efficiency of the single carrier (SC) system is extended to two dimensions, i.e., the time and frequency domains. Meanwhile, an optimization program is performed according to some criteria. As the precoding process may broaden the signal spectrum, we explicitly consider the spectrum mask as the constraint on the optimization, which makes our study more practical. Eventually, the minimum distance and capacity of the precoded FTN system are analyzed and compared with the traditional FTN system. With the degrees of freedom when constructing the precoder, the proposed scheme outperforms the FTN signaling schemes in terms of energy efficiency and noise immunity.

The rest of this paper is organized as follows. Section II briefly reviews the FTN system model. In Section III, the proposed FTN signaling scheme is presented, which is followed by the comprehensive performance analysis. In Section IV, the proposed optimization algorithm is investigated in the

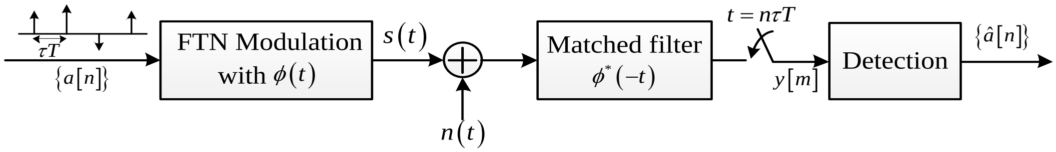

Fig. 1. Block diagram of the FTN-based transceiver system.

precoded FTN signal generation and simulation results verify the proposed scheme. Finally, some conclusions are drawn in Section V.

II. FTN System Model

In a SC communication system with linear modulation, let the vector $\mathbf{a} = \{a[n]\}$ and $\phi\left(t\right)$ be the i.i.d. input sequence and unit energy T-orthogonal pulse, respectively. Then the transmitted baseband signal can be expressed as

$$s\left(t\right) = \sum\nolimits_n a\left[n\right]\phi\left(t - n\tau T\right), \tag{1}$$

where τ is the packing ratio, and $0 < \tau \leq 1$. Since $\phi\left(t\right)$ follows the Nyquist criterion, the ISI-free detection can be implemented in a symbol-by-symbol manner when $\tau = 1$. For FTN signaling, however, the symbol duration is reduced to τT $(\tau < 1)$ for pursuing higher signaling rate, while yielding ISI unavoidably. As τ decreases, especially below the Mazo limit, more severe ISI is introduced. In other words, the capacity gain is obtained at the cost of increasing the computational complexity.

Subsequently, the FTN signal is passed through the additive white Gaussian noise (AWGN) channel with two-sided PSD $N_0/2$.[1] Let $v\left(t\right)$ be the colored noise generated by filtering $n\left(t\right)$, i.e., $v\left(t\right) = \int n\left(\lambda\right)\phi^*\left(\lambda - t\right)d\lambda$, then the matched filter outputs, sampled at the signaling rate, will be

$$y\left[m\right] = \sum\nolimits_n a\left[n\right]g\left[m - n\right] + v\left[m\right], \tag{2}$$

where $g_\phi\left[m\right] = \int \phi\left(\lambda\right)\phi^*\left(\lambda - m\tau T\right)d\lambda$ and $v\left[m\right] = v\left(m\tau T\right)$. Thereafter, the sample sequence $\mathbf{y}$ is fed into the trellis decoder to recover the transmitted data symbols. The block diagram of the FTN system is illustrated in Fig. 1.

Assuming the data symbols are wide-sense stationary, i.e.,

$$\begin{gathered}\mathrm{E}\left\{a\left[n\right]\right\} = 0\\ \mathrm{E}\left\{a\left[n\right]a^*\left[m\right]\right\} = \sigma_a^2\delta\left[m - n\right],\end{gathered}$$

where $\mathrm{E}\left\{\cdot\right\}$ and $\delta\left[n\right]$ denote the expectation operator and the Kronecker delta, respectively. Then, the PSD of the transmitted signal is given by [7]

$$\begin{aligned}S\left(f\right) &= \tfrac{1}{\tau T}\left|\psi\left(f\right)\right|^2\sum_k R_a\left(k\right)e^{-j2\pi fk\tau T}\\ &= \tfrac{\sigma_a^2}{\tau T}\left|\psi\left(f\right)\right|^2.\end{aligned} \tag{3}$$

[1]In this paper, we focus our attention on the precoder design at the transmitter under the assumption of AWGN channel. The interference introduced by the precoder indeed can be seen as a multi-path channels. Considering the physical multi-path fading channels is beyond the scope of this paper, which is left for the future study.

In (3), $\psi\left(f\right)$ is the Fourier transform of $\phi\left(t\right)$; R_a represents the autocorrelation function of $\mathbf{a}$, and here $R_a\left(k\right) = \sigma_a^2\delta[k]$. Neglecting the amplification on PSD by $1/\tau$, therefore, the PSD shape of the FTN signaling with i.i.d. inputs is governed by the shaping pulse.

III. High bandwidth-efficient precoded FTN signaling design

A. Precoded FTN Signal

Mathematically, the shape of the PSD in (3) is precisely determined by two factors. In practice, one popular method to control the PSD of the modulated signal, is through controlling $R_a\left(k\right)$ by introducing the predefined ISI. This precoding scheme is called as PRS, in which the purpose of the ISI is to shape the PSD for having a certain spectrum or bandwidth reduction. In this paper, the technique is combined with the legacy FTN systems for seeking a further increase of the spectral efficiency. Correspondingly, the new modulator structure is depicted in Fig. 2. Specifically, we take a convolutional precoding with the form

$$c\left[n\right] = \sum\nolimits_k a\left[n - k\right]b\left[k\right], \tag{4}$$

where $b\left[k\right]$ is the tap coefficient of the discrete-time filter with length $L_b + 1$. By exploiting the associativity of linear convolution, the signal generation in the precoded FTN system, works with a different shaping pulse $h\left(t\right)$, which is the combined response of $\mathbf{b} = \left\{b\left[k\right]\right\}$ and $\phi\left(t\right)$, i.e.,

$$h\left(t\right) = \sum_{n=0}^{L_b} b\left[n\right]\phi\left(t - n\tau T\right). \tag{5}$$

Substituting (4) into (3), the corresponding PSD of the precoded FTN signal is

$$\begin{aligned}S(f) &= \tfrac{\sigma_a^2}{\tau T}\left|\psi(f)\right|^2\left|\sum_{n=0}^{L_b} b[n]e^{-j2\pi fn\tau T}\right|^2\\ &= \tfrac{\sigma_a^2}{\tau T}\left|\psi(f)\right|^2\sum\nolimits_n g_b[n]e^{-j2\pi fn\tau T}\\ &= \tfrac{\sigma_a^2}{\tau T}\left|\psi(f)\right|^2 S_c\left(f\right),\end{aligned} \tag{6}$$

where $g_b\left[n\right] = \sum\nolimits_k b\left[k + n\right]b^*\left[k\right] = b\left[n\right] \star b^*\left[-n\right]$, and $\star$ denotes the convolution operator; $S_c\left(f\right)$ is the Fourier transform of $\mathbf{g}_b$. Moreover, the proportion of the bandwidth conservation from the precoder is defined as ζ. Hence, the method improving the spectral efficiency can be simultaneously carried out in the time and frequency domains. Given the τ and ζ, the data symbols are transmitted faster by a factor $1/\Upsilon$ with the same bandwidth, where the acceleration factor $\Upsilon = \tau\zeta$.

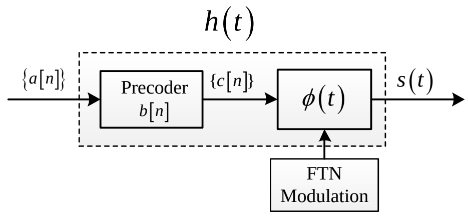

Fig. 2. Proposed bandwidth-efficient modulator structure.

B. Two Metrics: Minimum Distance and Capacity

As shown in (2), the sequence $\mathbf{y}$ is corrupted by lSI. According to [2], the asymptotic error probability with optimal detection (i.e., maximum-likelihood sequence estimation) at large E_b/N_0 is

$$P_e \approx K_1 Q\left(\sqrt{d_{\min}^2 E_b/N_0}\right), \tag{7}$$

where $Q(\cdot)$ is the cumulative Gaussian function, i.e., $Q(x) = \frac{1}{\sqrt{2\pi}}\int_x^{+\infty} e^{-t^2/2}dt, x>0$; K_1 is a weighting factor. Obviously, the noise immunity is closely involved in the normalized minimum distance, $d_{\min}$, which is defined as

$$\begin{aligned} d_{\min}^2 &= \min_{\mathbf{a}_1,\mathbf{a}_2:\mathbf{a}_1\neq\mathbf{a}_2} \tfrac{1}{2E_b}\int\left|s_{\mathbf{a}_1}(t)-s_{\mathbf{a}_2}(t)\right|^2 dt \\ &= \min_{\mathbf{e}=\mathbf{a}_1-\mathbf{a}_2\neq 0} \tfrac{1}{2E_b}\int\left|s_{\mathbf{e}}(t)\right|^2 dt = \min_{\mathbf{e}\neq 0}\tfrac{d^2(\mathbf{e})}{2E_b}, \end{aligned} \tag{8}$$

where $\mathbf{e}$ is referred to as an error event, and $d(\mathbf{e})$ denotes the distance of $\mathbf{e}$. The linear form of $d^2(\mathbf{e})$ is derived as follows [10]:

$$d^2(\mathbf{e}) = \sum\nolimits_n g_h[n]\,\rho_{\mathbf{e}}[n], \tag{9}$$

where $g_h[n] = \int h(\lambda)\,h^*(\lambda - n\tau T)\,d\lambda = g_b[n]\star g_\phi[n]$, and $\rho_{\mathbf{e}}[n] = \sum_k e[k+n]\,e[k]$. From (9), we can find $d_{\min}$ for $h(t)$ by searching over all legal $\rho_{\mathbf{e}}[n]$ sequences.

In addition to the minimum distance, the information rate is also a crucial target. For a given ISI channel with channel law $p(\mathbf{y}\,|\mathbf{a})$, the achievable information rate per output symbol, $I(\mathbf{a};\mathbf{y})$, between the input process $\mathbf{a} \triangleq \{a_1, a_2, \cdots, a_N\}$ and the output process $\mathbf{y} \triangleq \{y_1, y_2, \cdots, y_N\}$, is computed as

$$\begin{aligned} I(\mathbf{a};\mathbf{y}) &= \lim_{N\to\infty}\tfrac{1}{N}\left[H(\mathbf{y}) - H(\mathbf{y}\,|\mathbf{a})\right] \\ &= \lim_{N\to\infty}\tfrac{1}{N}\left\{\mathrm{E}\{-\log_2 p(\mathbf{y})\} - \mathrm{E}\{-\log_2 p(\mathbf{y}\,|\mathbf{a})\}\right\}, \end{aligned} \tag{10}$$

where $H(\cdot)$ is the N-dimensional differential entropy operator. Moreover, the channel capacity is defined as the maximum information rate.

For fixed transmission power P and shaping pulse $h(t)$, or equivalently signals with PSD $P|\psi(f)|^2 S_c(f)$ in (6), the capacity from Shannon theory equals

$$C_{shan.} = \int_0^W \log_2\left(\left[1+\frac{2P}{N_0}|\psi(f)|^2 S_c(f)\right]\right)df, \tag{11}$$

where W is the baseband bandwidth of $\phi(t)$. Similarly, the capacity of the precoded FTN signaling with Gaussian symbol distribution is given by [7]

$$C_{PFTN} = \int_0^{1/2\tau T} \log_2\left[1+\frac{2P}{N_0}|\psi_{fold}(f)|^2 S_c(f)\right]df, \tag{12}$$

where the subscript denotes precoded FTN. Meanwhile,

$$|\psi_{fold}(f)|^2 = \sum_k \left|\psi\left(f+\frac{k}{\tau T}\right)\right|^2, \ |f| \le 1/2\tau T \tag{13}$$

is called the folded spectrum of $|\psi(f)|^2$. Apparently, the optimal τ is $1/(2WT)$ such that the precoded FTN signal makes use of the PSD, and approaches the ultimate capacity $C_{shan.}$ in (11). For FTN signaling with i.i.d. inputs, i.e., $S_c(f) = 1$, hence, (12) reduces to

$$C_{FTN} = \int_0^{1/2\tau T} \log_2\left[1+\frac{2P}{N_0}|\psi_{fold}(f)|^2\right]df. \tag{14}$$

In the case of $\tau = 1$, (14) becomes

$$C_{Nyq.} = \frac{1}{2T}\log_2\left(1+\frac{2TP}{N_0}\right). \tag{15}$$

Eq. (15) actually is the capacity limit of Nyquist transmission schemes. In contrast to the preceding, however, there is no closed formula for the case of finite alphabet. In [12], a general Monte Carlo-based method is presented to accurately compute the information rate. Nevertheless, the complexity of the method increases exponentially with channel memory. Some researchers [13] focus on designing a filter to shorten the memory, and operate with a mismatched channel law $q(\mathbf{y}\,|\mathbf{a})$.

C. Optimal Precoder Design

High spectral efficiency can be obtained by using high-order modulation formats, while the performance is considerably sensitive to channel impairments such as the nonlinear effects and phase noise. In contrast, the low-order modulations are more robust in poor channel conditions. Motivated by this, the optimal precoded FTN signaling scheme is proposed for meeting the capacity requirements with employing a relatively low-order constellation. Meanwhile, in order to make a convenient and fair comparison with other two existing systems, i.e., the Nyquist and FTN systems, the basic shaping pulse $\phi(t)$ is fixed as a RRC pulse with 20% excess bandwidth. Therefore, the work is only concentrated on optimizing $\mathbf{b}$ under some special criteria and parameters.

In various transmission schemes, the transmitted signal should be restricted to meet specific constraints, such as the spectral requirements of the channel. Without loss of generality, here the 802.11g mask is considered as a restriction in the optimization process. The transmitted spectrum shall have a 0 dBr (i.e., dB relative to the maximum spectral density of the signal) bandwidth not exceeding 18 MHz and -20 dBr at 11 MHz frequency offset. The mask is depicted in Fig. 3. In operation, the frequency band is sampled. Let the sample points be the set Ξ, then $C(f_i) = S(f_i) - S_{mask}(f_i)$ denotes the spectrum gap between the normalized PSD described by (6) and the mask at frequency $f_i, f_i \in \Xi$.

Simultaneously, the optimal precoder configuration may comprise, e.g., raising $d_{\min}$ since Υ is lower than the Mazo limit; achieving a higher information rate; optimizing the passband ripple and stopband attenuation of $h(t)$. Nevertheless, the second objective is hardly executed because of its large calculation overhead. In this regard, an alternative target is to diminish the spectrum gap as much as possible to approach the ultimate capacity of the mask as close as possible. In this research, $d_{\min}$ and capacity are optimized simultaneously, which is a typical multi-objective optimization (also known as Pareto optimization [14]).

From an information theoretic point of view, however, the optimal distance characteristic may not simultaneously maximize the capacity [1], which implies that the optimal decisions need to be balanced between the two objectives. Since the introduced ISI should be eliminated effectively for ensuring the capacity gain, a simplified and feasible solution is only to maximize $d_{\min}$. Meanwhile, the capacity object is converted to a strong constraint, which actually is a predetermined threshold of the spectrum gap in passband.

For (6) and (9) are proportional to the autocorrelation $\mathbf{g}_b$, consequently the optimization could be carried out over $\mathbf{g}_b$. Accordingly, the admissibility constraints guaranteeing $\mathbf{g}_b$ valid are given by [10]

$$\sum\nolimits_n g_b[n] e^{-j2\pi nf} \geq 0, -1/2 \leq f \leq 1/2. \tag{16}$$

Finally, the problem of maximizing $d_{\min}$ subject to the spectrum mask and capacity, becomes a nonlinear constrained optimization, with standard formulation

$$\begin{aligned} & d^2_{\min,opt} = \max_{\mathbf{g}_b} \min_{\mathbf{e}} d^2(\mathbf{e}) \\ & s.t. \begin{cases} g_h[0] = 1 \\ satisfy \quad Ineq.\,(16) \\ c(f_i) = S(f_i) - S_{mask}(f_i) \leq 0, \forall f_i \in \Xi \\ \Gamma_0 \geq \Gamma = \frac{1}{|\Phi|} \sum\limits_{f_i \in \Phi} |c(f_i)|^2, \qquad \Phi \subset \Xi, \end{cases} \end{aligned} \tag{17}$$

where the elements of the set Φ are the sample points f_i in passband, and Γ_0 is the given threshold. Generally, $h(t)$ has unit energy, that's equivalent to $g_h[0] = \int |h(t)|^2 dt = 1$.

IV. Simulation Results

In this section, the 16-QAM signaling system performance in terms of noise immunity and spectral efficiency for $\Upsilon \in \{2/3, 1/2\}$ is investigated. These schemes, resulting in maximum information rates 3 and 4 bits per channel use as E_b/N_0 grows, can be regarded as the alternatives to 64, 256-QAM Nyquist systems, respectively. In the precoded FTN schemes, the two acceleration factors are analyzed into two parts: $\tau = 3/4, \zeta = 8/9$ and $\tau = 2/3, \zeta = 3/4$, respectively. The branch and bound algorithm [10] is utilized to calculate $d(\mathbf{e})$ in (17), by which the computational complexity is significantly reduced, in comparison with the exhaustive search. In addition, the MATLAB built-in routine fminimax.m has been applied directly to (17) for the optimal precoder. The corresponding precoders are listed as follows:

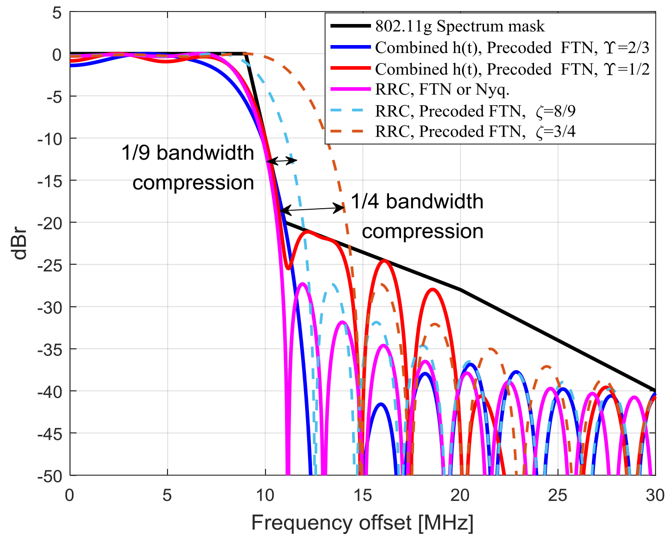

Fig. 3. Frequency domain reperesentation of the shaping pulses.

$$\mathbf{b} = \{-0.1134, -0.1456, 0.679, 0.7105\}$$

$$\begin{aligned} \mathbf{b} = \{&0.2048, -0.3447, 0.2512, -0.1393, 0.3608, -0.5292, \\ &-0.3866, -0.4439\} \end{aligned}$$

In the following, the simulation results are shown and discussed in depth. Meanwhile, the FTN system with the same spectral efficiency is adopted as a benchmark for comparison.

A. *Shaping Pulses of Precoded FTN system compared to Nyquist or FTN system*

Fig. 3 shows the frequency domain representation of the considered shaping pulses, including the basic shaping pulse $\phi(t)$ and the combined response $h(t)$. It is seen that the nominal bandwidth of $\phi(t)$ in the proposed scheme is $1/\zeta$ times that of used in the Nyquist or FTN system. Because the pre-expansion bandwidth is effectively compressed by the precoder, $h(t)$ still meets the mask limitations, resulting in a favorable response over most of the passband. Equivalently, a higher transmission rate is achieved with the same bandwidth.

B. *Noise immunity Performance of Precoded FTN system compared to FTN system*

The error events are searched out to length 30. The numerical results show that compared with the FTN signaling with $\tau = 2/3$, there is only around 0.2 dB gain from the precoder. When $\Upsilon = 1/2$, a considerable 2.8 dB gain is obtained with $d_{\min}$ from 0.131 [10] increase to 0.28.

C. *Spectral Efficiency Performance of Precoded FTN system compared to FTN system*

Fig. 4 exhibits the spectral efficiency of all considered schemes, as a function of E_b/N_0. The spectral efficiency here is accomplished by considering the 20% excess bandwidth paid for practical filtering characteristics. It can be observed both 64-QAM and 256-QAM Nyquist systems are bounded away from the Nyquist limit $C_{Nyq.}$ in (15), especially in the high-SNR regime. Moreover, although the same shaping pulse is used, there exists a certain gap between $C_{Nyq.}$ and the shannon capacity of RRC (this capacity coincides with C_{FTN} in (14) when $\tau \leq 1/(2WT)$). Hence, giving up the orthogonality condition opens an avenue for these systems with a finite input alphabet to pursue better performance.

Considering an approximation of the actually introduced ISI channel (i.e., an auxiliary channel [13]), the length of the ISI span is reduced to 10 for non-orthogonal schemes. The information rates are found with the Monte Carlo method. The results highlight that the 16-QAM precoded FTN signaling with $\Upsilon = 2/3$ achieves the spectral efficiency of 64-QAM orthogonal signaling, while the required E_b/N_0 is about 2.5 dB lower than its Nyquist counterpart. In addition, the proposed scheme has nearly identical performance to the 16-QAM FTN signaling with $\tau = 2/3$. Meanwhile, both break through the limit $C_{Nyq.}$.

When Υ is further reduced to 1/2, about 5 dB gain is obtained in comparison with 256-QAM Nyquist system. As demonstrated in the subfigure, the proposed scheme is also superior to the 16-QAM FTN signaling with $\tau = 1/2$, which is around 1 dB from the shannon capacity of RRC. Actually, for *M*-ary FTN signaling, the limit is achieved as the signaling rate tends to infinity [15]. Furthermore, the shannon capacity of $h(t)$, which equals to C_{PFTN} in (12) when $\tau \leq 1/(2WT)$, is larger than that of RRC, and approaches the ultimate capacity of the mask. Predictably, further capacity gain can be obtained as E_b/N_0 grows. Therefore, we boost the achievable capacity limit under the mask. In other words, compared with the legacy FTN system, the proposed FTN system is more suitable for high spectral efficiency requirements.

V. Conclusion

In this work, we have investigated the precoding technique in conjunction with the FTN-based system. A notable bandwidth can be conserved by introducing controlled ISI. The spectral efficiency is improved in both time and frequency domains. Meanwhile, the optimal precoder is explored under spectrum mask requirements. Simulation results demonstrate that in the proposed FTN system, the spectral efficiency of high-order constellation Nyquist system can be achieved by employing a low-order modulation. Moreover, the proposed scheme also outperforms the conventional FTN system. As the higher spectral efficiency, the superiority is clearer.

For moderate or large FTN rate (i.e., Υ is small and well below the Mazo limit), however, no efficient receivers can address well the severe ISI. This opens up for future work in receiver design. In the proposed scheme, Υ is decomposed into two parts that are within the Mazo limit. Therefore, employing a two-stage receiver to mitigate the ISI may be a feasible solution.

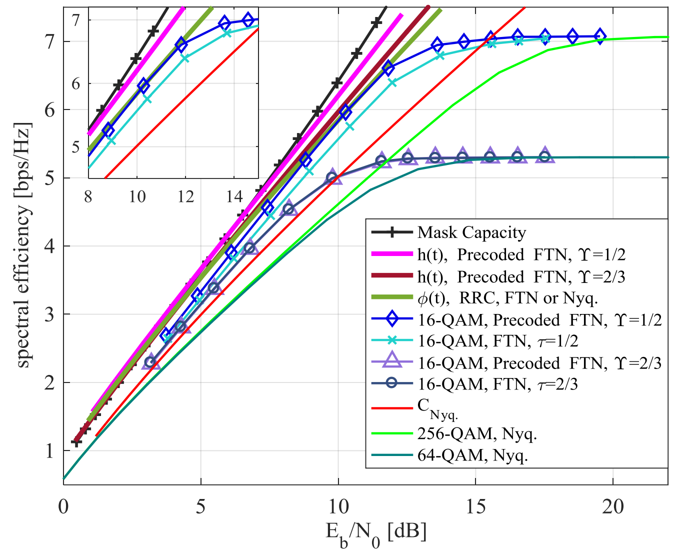

Fig. 4. The spectral efficiency comparison among the 16-QAM signaling with $\Upsilon = \{2/3, 1/2\}$ and 64, 256-QAM Nyqusit signaling. The heavy solid line is the shannon capacity with respect to the shaping pulse.

References

[1] J. Fan, S. Guo, X. Zhou *et al.*, “Faster-than-nyquist signaling: an overview,” *IEEE Access*, vol. 5, pp. 1925–1940, Feb. 2017.

[2] J. B. Anderson, F. Rusek, and V. Öwall, “Faster-than-nyquist signaling,” *Proc. IEEE*, vol. 101, no. 8, pp. 1817–1830, Aug. 2013.

[3] A. Modenini, F. Rusek, and G. Colavolpe, “Faster-than-nyquist signaling for next generation communication architectures,” in *Proc. 22nd Eur. Signal Process. Conf. (EUSIPCO)*, Lisbon, Portugal, Sept. 2014, pp. 1856–1860.

[4] F.-L. Luo and C. Zhang, *Signal Processing for 5G: Algorithms and Implementations*. John Wiley & Sons, 2016.

[5] J. Mazo, “Faster-than-nyquist signaling,” *Bell Syst. Tech. J.*, vol. 54, no. 8, pp. 1451–1462, 1975.

[6] A. D. Liveris and C. N. Georghiades, “Exploiting faster-than-nyquist signaling,” *IEEE Trans. Commun.*, vol. 51, no. 9, pp. 1502–1511, Sept. 2003.

[7] D. Kapetanovic and F. Rusek, “The effect of signaling rate on information rate for single carrier linear transmission systems,” *IEEE Trans. Commun.*, vol. 60, no. 2, pp. 421–428, Feb. 2012.

[8] A. Prlja and J. B. Anderson, “Reduced-complexity receivers for strongly narrowband intersymbol interference introduced by faster-than-nyquist signaling,” *IEEE Trans. Commun.*, vol. 60, no. 9, pp. 2591–2601, Sept. 2012.

[9] M. Jana, A. Medra, L. Lampe, and J. Mitra, “Pre-equalized faster-than-nyquist transmission,” *IEEE Trans. Commun.*, vol. 65, no. 10, pp. 4406–4418, May 2017.

[10] F. Rusek and J. B. Anderson, “Non binary and precoded faster than nyquist signaling,” *IEEE Trans. Commun.*, vol. 56, no. 5, pp. 808–817, May 2008.

[11] A. Said and J. B. Anderson, “Bandwidth-efficient coded modulation with optimized linear partial-response signals,” *IEEE Trans. Inf. Theory*, vol. 44, no. 2, pp. 701–713, Mar. 1998.

[12] D.-M. Arnold, H.-A. Loeliger, P. O. Vontobel, A. Kavcic, and W. Zeng, “Simulation-based computation of information rates for channels with memory,” *IEEE Trans. Inf. Theory*, vol. 52, no. 8, pp. 3498–3508, Aug. 2006.

[13] F. Rusek and D. Fertonani, “Bounds on the information rate of intersymbol interference channels based on mismatched receivers,” *IEEE Trans. Inf. Theory*, vol. 58, no. 3, pp. 1470–1482, Mar. 2012.

[14] R. E. Steuer, *Multiple criteria optimization: theory, computation, and applications*. Wiley, 1986.

[15] Y. G. Yoo and J. H. Cho, “Asymptotic optimality of binary faster-than-nyquist signaling,” *IEEE Commun. Lett.*, vol. 14, no. 9, pp. 788–790, Sept. 2010.